Shape evolution and collective dynamics of quasifission in the time-dependent Hartree-Fock approach

A. S. Umar,[1] V. E. Oberacker,[1] and C. Simenel[2]
[1]*Department of Physics and Astronomy, Vanderbilt University, Nashville, Tennessee 37235, USA*
[2]*Department of Nuclear Physics, RSPE, Australian National University, Canberra, ACT 0200, Australia*
(Received 23 June 2015; revised manuscript received 13 August 2015; published 28 August 2015)

Background: At energies near the Coulomb barrier, capture reactions in heavy-ion collisions result either in fusion or in quasifission. The former produces a compound nucleus in statistical equilibrium, while the second leads to a reseparation of the fragments after partial mass equilibration without formation of a compound nucleus. Extracting the compound nucleus formation probability is crucial to predict superheavy-element formation cross sections. It requires a good knowledge of the fragment angular distribution which itself depends on quantities such as moments of inertia and excitation energies which have so far been somewhat arbitrary for the quasifission contribution.
Purpose: Our main goal is to utilize the time-dependent Hartee-Fock (TDHF) approach to extract ingredients of the formula used in the analysis of experimental angular distributions. These include the moment-of-inertia and temperature.
Methods: We investigate the evolution of the nuclear density in TDHF calculations leading to quasifission. We study the dependence of the relevant quantities on various initial conditions of the reaction process.
Results: The evolution of the moment of inertia is clearly nontrivial and depends strongly on the characteristics of the collision. The temperature rises quickly when the kinetic energy is transformed into internal excitation. Then, it rises slowly during mass transfer.
Conclusions: Fully microscopic theories are useful to predict the complex evolution of quantities required in macroscopic models of quasifission.

DOI: 10.1103/PhysRevC.92.024621 PACS number(s): 21.60.Jz

I. INTRODUCTION

The creation of new elements is one of the most novel and challenging research areas of nuclear physics [1–4]. The search for a region of the nuclear chart that can sustain the so-called *superheavy elements* (SHE) has led to intense experimental activity resulting in the discovery and confirmation of elements with atomic numbers as large as $Z = 118$ [5–7]. The theoretically predicted *island of stability* in the SHE region of the nuclear chart is the result of new proton and neutron shell-closures, whose location is not precisely known [8–10]. The experiments to discover these new elements are notoriously difficult, with fusion evaporation residue (ER) cross section in picobarns. This cross section is commonly expressed in the product form

$$\sigma_{\rm ER} = \sum_{J=0}^{J_{\rm max}} \sigma_{\rm cap}(E_{\rm c.m.}, J) P_{\rm CN}(E^*, J) W_{\rm sur}(E^*, J), \qquad (1)$$

where $\sigma_{\rm cap}(E_{\rm c.m.}, J)$ is the capture cross section at center of mass energy $E_{\rm c.m.}$ and spin J. $P_{\rm CN}$ is the probability that the composite system fuses into a compound nucleus (CN) rather than breaks up via quasifission. $W_{\rm sur}$ is the survival probability of the fused system against fission. For light and medium mass systems the capture cross section may be considered to be the same as that for complete fusion. However, for heavy systems leading to superheavy formation, the ER cross section is dramatically reduced due to the quasifission and fusion-fission processes [11,12], thus making the capture cross section to be essentially the sum of these two cross sections.

The fusion process implies a transition from a dinuclear configuration—accompanied by particle exchange during the dynamical process—to a single-center compound-like configuration of the composite system. Most dynamical models [13–19] argue that, for heavy systems, a dinuclear complex is formed initially and the barrier structure and the excitation energy of this precompound system determine its survival to breaking up via quasifission. Furthermore, if the nucleus survives this initial state and evolves to a compound system, it can still fission due to its excitation.

Among the three stages towards ER given in Eq. (1), the determination of $P_{\rm CN}$ contains the most uncertainty which can be as much as 1–2 orders of magnitude [20,21]. Experimentally, $P_{\rm CN}$ can be extracted from the measurement of fusion-evaporation residue cross sections [22,23]. However, these cross sections become very small for heavy systems and the extraction of $P_{\rm CN}$ is uncertain for such systems. Information on $P_{\rm CN}$ can also be obtained by comparing the width of fragment mass distribution with the width expected in the case of pure fusion-fission [24,25]. This approach, however, only provides an upper limit for $P_{\rm CN}$ as it assumes that only fusion-fission produces symmetric fragments [24].

An alternative approach involves the analysis of the fragment angular distribution. For instance, assuming that the quasifission process, as fusion-fission, is statistical, the critical angular momentum $J_{\rm CN}$ between fusion-fission and quasifission can be adjusted to reproduce the experimental angular distribution of symmetric fragments [21,26,27]. Although this approach has been widely used, it could have limitations due to the fact that quasifission is not a statistical decay but a dynamical process, and that fusion-fission could be asymmetric due to, e.g., late-chance fusion-fission at low excitation energies [28] as well as shell structure of

pre-scission configurations [29]. Correlations between mass and scattering angle of the fragments have also been measured extensively [25,30–33]. In particular, they can be used to disentangle fast quasifission processes (few zeptoseconds) to longer reaction mechanisms associated with contact times between the fragments exceeding 10–20 zs (i.e., long-time quasifission and fusion-fission). However, the analysis of such fragment mass-angle distributions [30,31], as well as statistical descriptions of fragment angular distributions [26], require external parameters such as moment of inertia and temperature which are chosen somewhat arbitrarily [21,26,34]. It is therefore important to provide a realistic evaluation of these parameters, in particular for the quasifission mechanism which requires a description of the complex nuclear dynamics.

Dynamical microscopic approaches are a standard tool to extract macroscopic properties in heavy-ion collisions [35–39]. In particular, the time-dependent Hartree-Fock theory [40], has been recognized for its realistic description of several low-energy nuclear reaction mechanisms [41,42]. It has been recently utilized for studying the dynamics of quasifission [25,33,43,44] and scission [45–47]. The study of quasifission is showing a great promise to provide insight based on very favorable comparisons with experimental data [25,33]. As a dynamical microscopic theory, TDHF provides us with the complete shape evolution of the nuclear densities which can be used to compute the time evolution of deformation and inertia parameters. Using an extension to TDHF, the so-called density constraint TDHF (DC-TDHF) approach [35], it is also possible to compute the excitation energy in the fragments.

In this paper we focus our discussion on the extraction of the time evolution of the moment of inertia and of the excitation energy (temperature). These are indeed the relevant quantities for fragment mass-angle distributions and angular distribution analyses. These quantities are computed for collisions between calcium isotopes and actinides for which the TDHF approach has been shown to provide a deep insight into the quasifission reaction mechanisms [33,43,44].

II. FORMALISM

A. TDHF and DC-TDHF approaches

The theoretical formalism for the microscopic description of complex many-body quantum systems and the understanding of the nuclear interactions that result in self-bound, composite nuclei possessing the observed properties are the underlying challenges for studying low energy nuclear physics. The Hartree-Fock approximation and its time-dependent generalization, the time-dependent Hartree-Fock theory, have provided a possible means to study the diverse phenomena observed in low energy nuclear physics [41,42]. In general modern TDHF calculations provide a useful foundation for a fully microscopic many-body description of large amplitude collective motion including collective surface vibrations and giant resonances [48–61] nuclear reactions in the vicinity of the Coulomb barrier, such as fusion [36,39,62–69], deep-inelastic reactions and transfer [70–76], and dynamics of (quasi)fission fragments [33,43–47].

Despite its successes, the TDHF approach has important limitations. In particular, it assumes that the many-body state remains a single Slater determinant at all times. It describes the time-evolution of an independent particle system in a single mean-field corresponding to the dominant reaction channel. As a result, it induces a classical behavior of many-body observables. A well-known example is that TDHF does not include tunneling of the many-body wave function and, thus, it is unable to describe sub-barrier fusion. It also underestimates the width of fragment mass and charge distributions in strongly dissipative collisions [70,72,77]. Thus, to obtain multiple reaction channels or widths of one-body observables one must in principle go beyond TDHF [72,78–81].

In fact, different reaction outcomes can also be obtained from mean-field calculations if the initial state (defined by the center of mass energy $E_{\rm c.m.}$ and by the orbital angular momentum L of the collision) is best described by a superposition of independent (quasi)particle states and that each of these states can be assumed to evolve in its own mean field. This is the case, for instance, if a collision partner is deformed in its intrinsic frame. In this case, each orientation of the deformed nucleus may encounter a different mean-field evolution [82,83]. Such orientation dependence of reaction mechanisms has been experimentally studied in quasifission with actinide targets [84–90] and confirmed in TDHF studies [25,33,42]. In particular, these studies have shown that collisions of a spherical projectile with the tip of prolately deformed actinides lead to fast quasifission (with contact time smaller than 10 zs) while collisions with the side of the actinide may induce longer contact times, larger mass transfer, and possible fusion. It is therefore common practice to investigate a subset of specific orientations depending on the reaction mechanism one is interested in investigating. For instance, it is sufficient to study "side collisions" in order to investigate the competition between quasifission and fusion in collisions with actinide nuclei [43].

In recent years it has become numerically feasible to perform TDHF calculations on a 3D Cartesian grid without any symmetry restrictions and with much more accurate numerical methods [42,52,74,91–93]. In addition, the quality of effective interactions has been substantially improved [94–97]. In order to overcome the lack of quantum tunneling preventing direct studies of sub-barrier fusion, the DC-TDHF method was developed to compute heavy-ion potentials [35] and excitation energies [98] directly from TDHF time-evolution. For instance, this method was applied to calculate capture cross sections for hot and cold fusion reactions leading to superheavy element $Z = 112$ [65].

B. Fragment angular distributions

Experimental analysis of the fragment angular distributions $W(\theta)$ is commonly expressed in terms of a two-component expression for fusion-fission and quasifission parts [26,27,99–101],

$$W(\theta) = \sum_{J=0}^{J_{\rm CN}} \mathcal{F}_J^{(FF)}(\theta) + \sum_{J=J_{\rm CN}}^{J_{\rm max}} \mathcal{F}_J^{(QF)}(\theta), \qquad (2)$$

where

$$\mathcal{F}_J^{(\alpha)} = \frac{(2J+1)^2 \exp\left[-(J+1/2)^2 \sin^2\theta/4K_0^2(\alpha)\right] J_0\left[i(J+1/2)^2 \sin^2\theta/4K_0^2(\alpha)\right]}{\mathrm{erf}\left[(J+1/2)/\left(2K_0^2(\alpha)\right)^{1/2}\right]} \tag{3}$$

and $\alpha \equiv$ FF (fusion-fission) or QF (quasifission). Here, $J_{\rm CN}$ defines the boundary between fusion-fission and quasifission, assuming a sharp cutoff between the angular momentum distributions of each mechanism. The detailed definition of various mathematical functions can be found in Refs. [21,99].

The quantum number K is known to play an important role in fission [102]. The latter is defined as the projection of the total angular momentum along the deformation axis. In the transition state model (TSM) [102], the characteristics of the fission fragments are determined by the K distribution at scission. The argument K_0 entering Eq. (3) is the width of this distribution which is assumed to be Gaussian. It obeys

$$K_0^2 = T\Im_{\rm eff}/\hbar^2 , \tag{4}$$

where the effective moment of inertia, $\Im_{\rm eff}$, is computed from the moments of inertia for rotations around the axis parallel and perpendicular to the principal deformation axis

$$\frac{1}{\Im_{\rm eff}} = \frac{1}{\Im_{\parallel}} - \frac{1}{\Im_{\perp}} , \tag{5}$$

and T is the nuclear temperature at the saddle point. The physical parameters of the fusion-fission part are relatively well known from the liquid-drop model [103,104]. In contrast, the quasifission process never reaches statistical equilibrium. In principle, it has to be treated dynamically, while Eq. (3) is based on a statistical approximation. In addition, the usual choice for the nuclear moment of inertia for the quasifission component, $\Im_0/\Im_{\rm eff} = 1.5$ [21,26,34], is somewhat arbitrary.

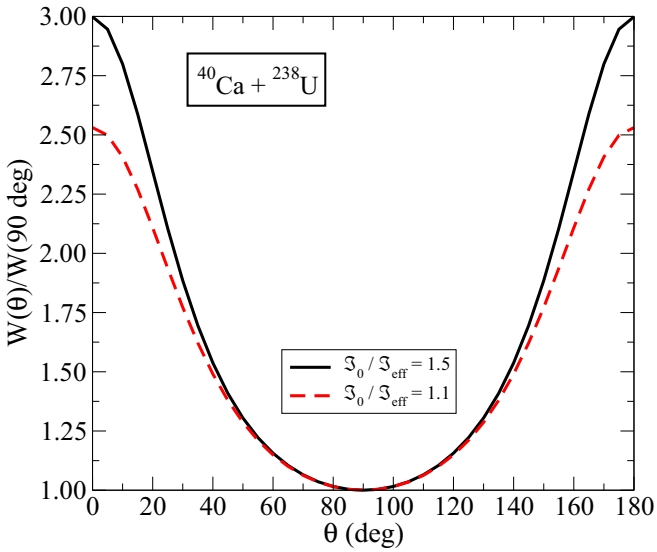

FIG. 1. (Color online) Effect of the moment of inertia on the angular distribution of the fragments computed with Eqs. (2) and (3). Both curves were calculated using $J_{\rm CN} = 46$ and $T = 1.2$ MeV.

Here, $\Im_0$ is the moment of inertia of an equivalent spherical nucleus.

In order to illustrate the sensitivity of the fragment angular distribution with the chosen value of the moment of inertia, we have plotted the ratio $W(\theta)/W(90^\circ)$ in Fig. 1 with $\Im_0/\Im_{\rm eff} = 1.1$ and 1.5. Here, we used the value of $J_{\rm CN} = 46$ obtained directly from TDHF calculations of quasifission for this system. Similarly, temperature was taken to be $T = 1.2$ MeV. The deviation is mostly visible at most forward and backward angles, where it can reach up to 20%. It is interesting to note that if we assume that the red dashed curve of Fig. 1 is the actual measured quantity and try to fit it by varying the $J_{\rm CN}$ value of the black solid curve we obtain a value of $J_{\rm CN} = 37$. This would then be the error for using the wrong $J_{\rm CN}$ value.

In the following section we outline the extraction of these ingredients directly from TDHF time-evolution of collisions resulting in quasifission.

III. RESULTS

The feasibility of using TDHF for quasifission has only been recognized recently [33,42,43]. By virtue of long contact times for quasifission and the energy, orientation, and impact parameter dependencies, these calculations require extremely long CPU times and numerical accuracy [91–93,105]. During the collision process, the nuclear densities, as described by TDHF time-evolution, undergo complicated shape changes including vibration and rotation. Such evolutions finally lead to two separated final fragments identified as quasifission due to the long contact-time for the reaction as well as the mass/charge of the fragments [33,43].

In Fig. 2 we show a few time snapshots of the evolving mass density for the QF reaction of the ^{48}Ca + ^{249}Bk system

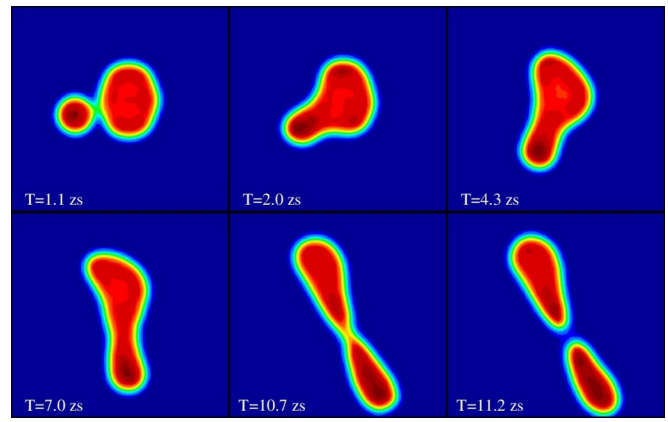

FIG. 2. (Color online) Quasifission in the reaction ^{48}Ca + ^{249}Bk at $E_{\rm c.m.} = 218$ MeV with impact parameter $b = 2.0$ fm. Shown is a contour plot of the time evolution of the mass density. The actual numerical box is larger than the one shown in the frames.

at $E_{\text{c.m.}} = 218$ MeV with impact parameter $b = 2.0$ fm. The times are given in zeptoseconds ($1\,\text{zs} = 10^{-21}\text{s}$). Our HF/TDHF code contains all of the time-odd terms present in the Skyrme interaction and does not impose time-reversal invariance. Each nucleon is represented by a two-component spinor. TDHF calculations always contain time-odd terms as these are nonzero for time evolution and guarantee Galilean invariance. Consequently, we are able to directly compute odd systems without resorting to filling type approximations. The very large elongation of the separating fragments is noteworthy. The initial orientation of the deformed ^{249}Bk was chosen such that the spherical ^{48}Ca nucleus collides with the side of the actinide nucleus. In the following we will refer to this as the "side" orientation.

A. Incoming and outgoing potentials

As quasifission is part of the capture process, it is therefore possible to compute the nucleus-nucleus potential down to the inside barrier region with the DC-TDHF technique. The latter is represented in Fig. 3 for the incoming channel of a $^{40}\text{Ca} + ^{238}\text{U}$ central collision. After contact, the two fragments encounter a significant mass transfer toward symmetry. The outgoing potential is therefore different than the incoming one. In fact, the outgoing potential does not exhibit any barrier, leading to a reseparation of the fragments. The representation of the ion-ion potential in terms of the separation distance R is well defined during the entrance channel phase of the collision. For the outgoing channel, the dynamical change of the neck position during the overlap phase causes the observed oscillations in the potential energy curve. After the nuclei form a more compact system the representation in terms of a single coordinate R is no longer adequate since the system now is moving in a multidimensional potential energy surface and the interpretation of this part of the potential should be considered in this context.

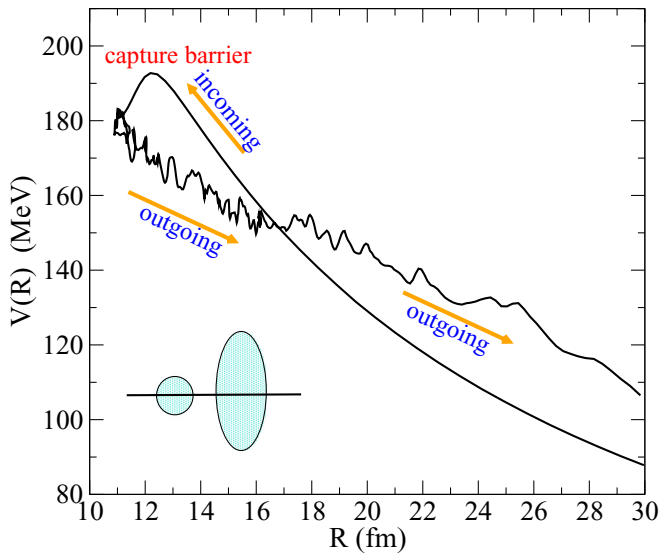

FIG. 3. (Color online) DC-TDHF nucleus-nucleus potential for the $^{40}\text{Ca} + ^{238}\text{U}$ central collision at $E_{\text{c.m.}} = 211$ MeV and with the side orientation. Both the potentials for the incoming and outgoing channels are shown.

B. Moment of inertia

The first collective observable of interest for fission and quasifission (both dynamical and statistical) studies is the moment of inertia of the system. The proper way to calculate the moment-of-inertia for such time-dependent densities (particularly for nonzero impact parameters) is to directly diagonalize the moment-of-inertia tensor represented by a 3×3 matrix with elements

$$\Im_{ij}(t)/m = \int d^3r\ \rho(\mathbf{r},t)(r^2\delta_{ij} - x_i x_j)\ , \tag{6}$$

where ρ is the local number density calculated from TDHF evolution, m is the nucleon mass, and $x_{i=1,2,3}$ denote the Cartesian coordinates. The TDHF calculations are done in three-dimensional Cartesian geometry [92]. Numerical diagonalization the matrix $\Im$ gives three eigenvalues. One eigenvalue corresponds to the moment-of-inertia $\Im_{\parallel}$ for the nuclear system rotating about the principal axis. The other two eigenvalues define the moments of inertia for rotations about axes perpendicular to the principal axis. Naturally, for triaxial density distributions, the two perpendicular components are not exactly equal but for practical calculations they are close enough and always larger than the parallel component. We thus use a single average value for these moments of inertia denoted by $\Im_{\perp}$.

Using the time-dependent moment-of-inertia obtained from the TDHF collision one can calculate the so-called effective moment-of-inertia defined in Eq. (5). It is standard to compute the effective moment of inertia relative to a spherical system using the mass independent quantity $\Im_0/\Im_{\text{eff}}$, where $\Im_0$ is the moment-of-inertia of a spherical nucleus with the same number of nucleons [21,27]. The expression for the moment-of-inertia for a rigid sphere is given by $\Im_0/m = 2AR_0^2/5$, where R_0 can be chosen as $R_0 = 1.225A^{1/3}$ fm [27].

1. Role of impact parameter

The moment-of-inertia ratio calculated for the $^{48}\text{Ca} + ^{249}\text{Bk}$ noncentral collisions at $E_{\text{c.m.}} = 218$ MeV is shown in Fig. 4. These trajectories all lead to quasifission with a large mass transfer and orbiting before the separation of the fragments. This is illustrated in Fig. 2 for the impact parameter $b = 2$ fm case. For this system using the value of $\hbar^2/m = 41.471$ MeV fm^2 and total mass number $A = 297$, we get $\Im_0 = 191.359\hbar^2$ MeV^{-1}. At the point of final touching configuration the moment-of-inertia ratios are in the range 1.4–1.8, suggesting a relatively strong impact parameter dependence. Impact parameters smaller than $b = 0.5$ fm lead to contact time between the fragments exceeding 35 zs. We can therefore consider that the nuclei have fused and would ultimately form a compound nucleus. The atypical value of the moment of inertia ratio for the $b = 2$ fm case of Fig. 4 can be understood by the examination of the contact time for quasifission, which shows an increase at $b = 2$ fm region compared to the smaller and larger impact parameters. This is also manifested as the region where the light fragment is a

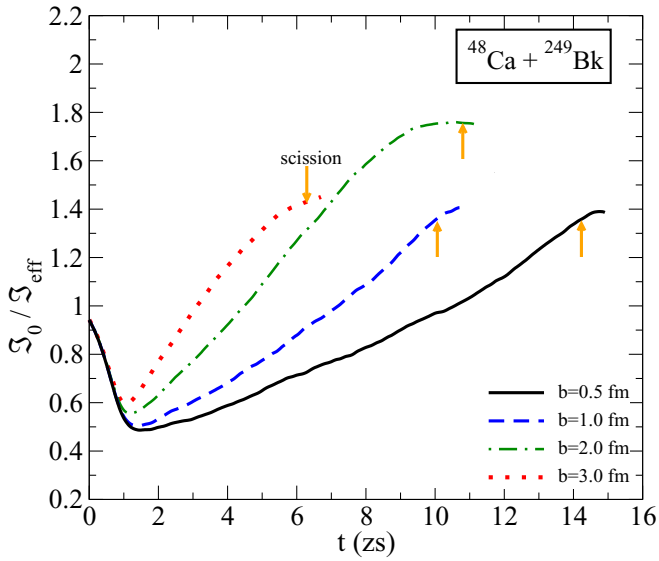

FIG. 4. (Color online) TDHF results showing the time-dependence of the ratio $\Im_0/\Im_{\rm eff}$ for the ^{48}Ca + ^{249}Bk system at $E_{\rm c.m.} = 218$ MeV and for impact parameters ranging from $b = 0.5$ to 3 fm. The arrows indicate the scission point of each trajectory.

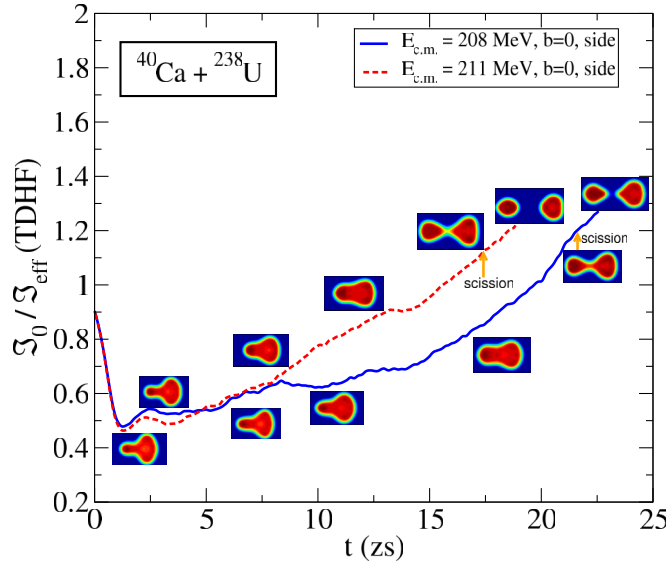

FIG. 5. (Color online) TDHF results showing the time-dependence of the ratio $\Im_0/\Im_{\rm eff}$ for the ^{40}Ca + ^{238}U system at energies $E_{\rm c.m.} = 208$ (solid blue curve) and 211 MeV (dashed red curve) for zero impact parameter.

neutron rich Zr isotope with $A \approx 102$–106. The microscopic evolution of the shell structure seems to have a tendency to form a composite with a longer lifetime when the light fragment is in this region. This was also discussed for the case of the ^{40,48}Ca + ^{238}U quasifission study of Ref. [43]. In Ref. [43] this was explained as being due to the presence of strongly bound deformed isotopes of Zr in this region [106].

2. Role of center-of-mass energy

Next we consider central collisions of the ^{40}Ca + ^{238}U systems. Similar to the ^{249}Bk case, ^{238}U exhibits a strong prolate deformation and its alignment with respect to the collision axis changes the quasifission characteristics [33]. The value of $\Im_0$ is 171.394 $\hbar^2$ MeV^{-1} for $A = 278$.

Figure 5 shows the time-evolution of the moment-of-inertia ratio at two different center-of-mass energies for central collisions with the side orientation. The two calculations have an energy difference of only 3 MeV in order to compare reactions which lead to similar mass asymmetry of the fragments. It is interesting to observe that up to ∼8 zs, the two evolutions of the moment of inertia are almost identical. This is likely to be due to the fact that the translational kinetic energy is rapidly dissipated in both cases, leading to a system with similar compactness but different excitation energies. For longer times, we observe a faster reseparation of the fragments at the highest center-of-mass energy. However, the final value of the ratio $\Im_0/\Im_{\rm eff} \simeq 1.2$ is approximately the same for both energies. Note that this value is again different from the assumed ratio of 1.5.

3. Role of the orientation

Figure 6 shows the dependence of the moment-of-inertia ratio on the orientation of the ^{238}U nucleus for the ^{48}Ca + ^{238}U system ($\Im_0 = 179.693\ \hbar^2$ MeV^{-1} for $A = 286$). The shorter contact time for the tip orientation (elongation axis of ^{238}U parallel to the collision axis) is evident from the figure. We also observe that at the initial contact and for most of the evolution, the ratios are significantly different, originating from the very different initial density configurations. However, as the two reactions approach the scission point the ratios become relatively close to one another: The neck breaks at $\Im_0/\Im_{\rm eff} \sim 1.1$–$1.2$. These values are, again, significantly smaller than the assumed value of 1.5.

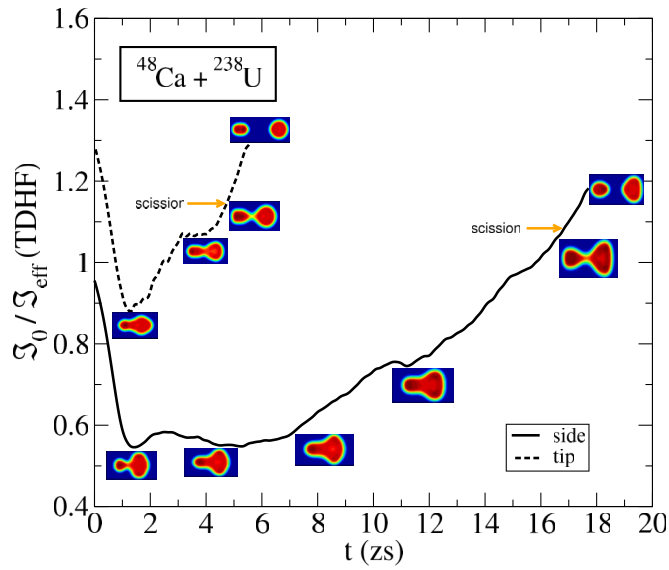

FIG. 6. (Color online) TDHF results showing the time-dependence of the ratio $\Im_0/\Im_{\rm eff}$ for the ^{48}Ca + ^{238}U system at energy $E_{\rm c.m.} = 203$ MeV for zero impact parameter and two orientations of the ^{238}U nucleus.

C. Collective dynamics and temperature

In this section we study the evolution of the TDHF density relative to the dynamical potential energy surface (PES) using the DC-TDHF method. In the DC-TDHF method a parallel static calculation is performed at given time intervals which constrains the instantaneous TDHF density and finds the corresponding minimum energy state. This allows us to trace the TDHF dynamical trajectory on the PES, albeit restricted to the shapes calculated in TDHF evolution. At the same time these calculations provide the dynamical excitation energy, $E^*(t)$ [98]. The DC-TDHF calculations for heavy systems are extremely compute extensive and the calculation of the trajectories performed here took about two months of computing on a 16-processor modern workstation utilizing all processors.

The temperature used in Eq. (4) is taken to be the temperature at the saddle point of a fissioning system [21,34]. Since this is adopted from the modeling of fission it may not be appropriate for quasifission, which does not really have a saddle point in the sense of ordinary fission and it is a fully dynamical process.

We have computed the dynamical temperature of the system during the quasifission path using the calculated excitation energy, $E^*(t)$, as $T(t) = \sqrt{E^*(t)/(A/8.5)}$ in MeV. Figure 7(a) shows the TDHF results for the ^{40}Ca $+^{238}$U central collision at $E_{\text{c.m.}} = 211$ MeV and side orientation. We see that the temperature rapidly rises during the initial overlap phase of the collision and reaches a value of about 1.0 MeV. After this the temperature rises more slowly being in the range of 1.25–1.5 MeV along the scission path. In Fig. 7(b) we show the change of the width of the K distribution, K_0^2 of Eq. (4), as a function of time for the same system. After the initial rise K_0^2 gradually decreases for later times. This decrease is a result of the interplay between temperature, which rises as a function of time, and the effective moment of inertia, which decreases at a slightly faster rate. The decrease of the effective moment of inertia can be inferred from the rising value for the ratio $\Im_0/\Im_{\text{eff}}$, with $\Im_0$ being a constant.

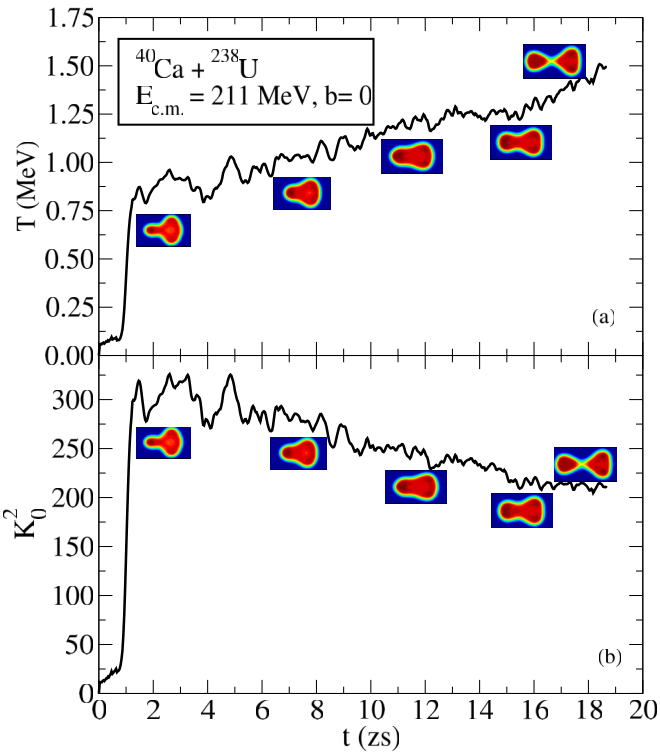

FIG. 7. (Color online) (a) TDHF results showing the time-dependence of the temperature for the ^{40}Ca $+^{238}$U system at energy $E_{\text{c.m.}} = 211$ MeV for zero impact parameter and side orientation of the ^{238}U nucleus. (b) The change of the width of the K distribution, K_0^2 of Eq. (4), as a function of time for the same system.

While the calculation of the full temperature dynamics is very computationally expensive one can calculate the temperature if the dynamical density is stored at a chosen time. This would then allow us to obtain all the ingredients of the parameter K_0 of Eq. (4). One problem is that so far we do not have a convention for knowing exactly at what point one is supposed to evaluate the ingredients of K_0. The closest configuration to a fission saddle point would be the most compact shape formed just after full dissipation of the translational kinetic energy. In this case, this would correspond to the end of the first, fast rise of $T(t)$, with a value of $\sim$1 MeV.

IV. SUMMARY

The fully microscopic TDHF theory has shown itself to be rich in nuclear phenomena and continues to stimulate our understanding of nuclear dynamics. We have used the TDHF theory to study evolution of the nuclear density for reactions resulting in quasifission with a focus on the ingredients that are used to analyze experimental angular distributions to calculate the fusion probability P_{CN}. We show that a number of useful quantities can be obtained from TDHF dynamics rather than utilizing models that may not be appropriate for quasifission. Among these are the moment-of-inertia parallel and perpendicular to the symmetry axis, temperature through the calculation of the dynamical excitation energy, as well as other quantities like the rotational energy. In addition TDHF can tell us the dependence of these variables on impact parameter, energy, and structure. Future studies will involve the calculation of the P_{CN} using TDHF calculations in connection with the experimental data of Ref. [25]. In this study we also plan to utilize the mass-angle distributions obtained directly from TDHF.

Finally, we should keep in mind that TDHF evolutions may be complex and thus the resulting trajectories could depend on numerical approximations as well as on the choice of the effective interaction. In particular, the effect of the latter on P_{CN} predictions should be carefully investigated.

ACKNOWLEDGMENTS

We thank W. Loveland and D. J. Hinde for stimulating discussions. This work has been supported by the U.S. Department of Energy under Grant No. DE-SC0013847 with Vanderbilt University and by the Australian Research Council Grant No. FT120100760.

[1] P. Armbruster, Ann. Rev. Nucl. Part. Sci. **35**, 135 (1985).
[2] S. Hofmann, Rep. Prog. Phys. **61**, 639 (1998).
[3] S. Hofmann and G. Münzenberg, Rev. Mod. Phys. **72**, 733 (2000).
[4] Yuri Oganessian, J. Phys. G **34**, R165 (2007).
[5] Yu. Ts. Oganessian, F. Sh. Abdullin, P. D. Bailey, D. E. Benker, M. E. Bennett, S. N. Dmitriev, J. G. Ezold, J. H. Hamilton, R. A. Henderson, M. G. Itkis, Yu. V. Lobanov, A. N. Mezentsev, K. J. Moody, S. L. Nelson, A. N. Polyakov, C. E. Porter, A. V. Ramayya, F. D. Riley, J. B. Roberto, M. A. Ryabinin, K. P. Rykaczewski, R. N. Sagaidak, D. A. Shaughnessy, I. V. Shirokovsky, M. A. Stoyer, V. G. Subbotin, R. Sudowe, A. M. Sukhov, Yu. S. Tsyganov, V. K. Utyonkov, A. A. Voinov, G. K. Vostokin, and P. A. Wilk, Phys. Rev. Lett. **104**, 142502 (2010).
[6] Yu. Ts. Oganessian, F. Sh. Abdullin, C. Alexander, J. Binder, R. A. Boll, S. N. Dmitriev, J. Ezold, K. Felker, J. M. Gostic, R. K. Grzywacz, J. H. Hamilton, R. A. Henderson, M. G. Itkis, K. Miernik, D. Miller, K. J. Moody, A. N. Polyakov, A. V. Ramayya, J. B. Roberto, M. A. Ryabinin, K. P. Rykaczewski, R. N. Sagaidak, D. A. Shaughnessy, I. V. Shirokovsky, M. V. Shumeiko, M. A. Stoyer, N. J. Stoyer, V. G. Subbotin, A. M. Sukhov, Yu. S. Tsyganov, V. K. Utyonkov, A. A. Voinov, and G. K. Vostokin, Phys. Rev. Lett. **109**, 162501 (2012).
[7] J. Khuyagbaatar, A. Yakushev, Ch. E. Düllmann, D. Ackermann, L.-L. Andersson, M. Asai, M. Block, R. A. Boll, H. Brand, D. M. Cox, M. Dasgupta, X. Derkx, A. Di Nitto, K. Eberhardt, J. Even, M. Evers, C. Fahlander, U. Forsberg, J. M. Gates, N. Gharibyan, P. Golubev, K. E. Gregorich, J. H. Hamilton, W. Hartmann, R.-D. Herzberg, F. P. Heßberger, D. J. Hinde, J. Hoffmann, R. Hollinger, A. Hübner, E. Jäger, B. Kindler, J. V. Kratz, J. Krier, N. Kurz, M. Laatiaoui, S. Lahiri, R. Lang, B. Lommel, M. Maiti, K. Miernik, S. Minami, A. Mistry, C. Mokry, H. Nitsche, J. P. Omtvedt, G. K. Pang, P. Papadakis, D. Renisch, J. Roberto, D. Rudolph, J. Runke, K. P. Rykaczewski, L. G. Sarmiento, M. Schädel, B. Schausten, A. Semchenkov, D. A. Shaughnessy, P. Steinegger, J. Steiner, E. E. Tereshatov, P. Thörle-Pospiech, K. Tinschert, T. Torres De Heidenreich, N. Trautmann, A. Türler, J. Uusitalo, D. E. Ward, M. Wegrzecki, N. Wiehl, S. M. Van Cleve, and V. Yakusheva, Phys. Rev. Lett. **112**, 172501 (2014).
[8] M. Bender, K. Rutz, P.-G. Reinhard, J. A. Maruhn, and W. Greiner, Phys. Rev. C **60**, 034304 (1999).
[9] A. Staszczak, A. Baran, and W. Nazarewicz, Phys. Rev. C **87**, 024320 (2013).
[10] S. Ćwiok, P.-H. Heenen, and W. Nazarewicz, Nature **433**, 705 (2005).
[11] C.-C. Sahm, H.-G. Clerc, K.-H. Schmidt, W. Reisdorf, P. Armbruster, F. P. Heßberger, J. G. Keller, G. Münzenberg, and D. Vermeulen, Z. Phys. A **319**, 113 (1984).
[12] K.-H. Schmidt and W. Morawek, Rep. Prog. Phys. **54**, 949 (1991).
[13] G. Fazio, G. Giardina, G. Mandaglio, R. Ruggeri, A. I. Muminov, A. K. Nasirov, Y. T. Oganessian, A. G. Popeko, R. N. Sagaidak, A. V. Yeremin, S. Hofmann, F. Hanappe, and C. Stodel, Phys. Rev. C **72**, 064614 (2005).
[14] G. G. Adamian, N. V. Antonenko, and W. Scheid, Phys. Rev. C **68**, 034601 (2003).
[15] A. K. Nasirov, G. Giardina, G. Mandaglio, M. Manganaro, F. Hanappe, S. Heinz, S. Hofmann, A. I. Muminov, and W. Scheid, Phys. Rev. C **79**, 024606 (2009).
[16] G. G. Adamian, N. V. Antonenko, and W. Scheid, Eur. Phys. J. A **41**, 235 (2009).
[17] Z.-Q. Feng, G.-M. Jin, J.-Q. Li, and W. Scheid, Nucl. Phys. A **816**, 33 (2009).
[18] V. Zagrebaev and W. Greiner, J. Phys. G **34**, 2265 (2007).
[19] Y. Aritomo, Phys. Rev. C **80**, 064604 (2009).
[20] W. Loveland, Phys. Rev. C **76**, 014612 (2007).
[21] R. Yanez, W. Loveland, J. S. Barrett, L. Yao, B. B. Back, S. Zhu, and T. L. Khoo, Phys. Rev. C **88**, 014606 (2013).
[22] A. C. Berriman, D. J. Hinde, M. Dasgupta, C. R. Morton, R. D. Butt, and J. O. Newton, Nature **413**, 144 (2001).
[23] J. Khuyagbaatar, K. Nishio, S. Hofmann, D. Ackermann, M. Block, S. Heinz, F. P. Heßberger, K. Hirose, H. Ikezoe, B. Kinlder, B. Lommel, H. Makii, S. Mitsuoka, I. Nishinaka, T. Ohtsuki, Y. Wakabayashi, and S. Yan, Phys. Rev. C **86**, 064602 (2012).
[24] C. J. Lin, R. du Rietz, D. J. Hinde, M. Dasgupta, R. G. Thomas, M. L. Brown, M. Evers, L. R. Gasques, and M. D. Rodriguez, Phys. Rev. C **85**, 014611 (2012).
[25] K. Hammerton, Z. Kohley, D. J. Hinde, M. Dasgupta, A. Wakhle, E. Williams, V. E. Oberacker, A. S. Umar, I. P. Carter, K. J. Cook, J. Greene, D. Y. Jeung, D. H. Luong, S. D. McNeil, C. S. Palshetkar, D. C. Rafferty, C. Simenel, and K. Stiefel, Phys. Rev. C **91**, 041602 (2015).
[26] B. B. Back, Phys. Rev. C **31**, 2104 (1985).
[27] M. B. Tsang, H. Utsunomiya, C. K. Gelbke, W. G. Lynch, B. B. Back, S. Saini, P. A. Baisden, and M. A. McMahan, Phys. Lett. B **129**, 18 (1983).
[28] J. Khuyagbaatar, D. J. Hinde, I. P. Carter, M. Dasgupta, Ch. E. Düllmann, M. Evers, D. H. Luong, R. du Rietz, A. Wakhle, E. Williams, and A. Yakushev, Phys. Rev. C **91**, 054608 (2015).
[29] J. D. McDonnell, W. Nazarewicz, J. A. Sheikh, A. Staszczak, and M. Warda, Phys. Rev. C **90**, 021302(R) (2014).
[30] J. Töke, R. Bock, G. X. Dai, A. Gobbi, S. Gralla, K. D. Hildenbrand, J. Kuzminski, W. F. J. Müller, A. Olmi, H. Stelzer, B. B. Back, and S. Bjørnholm, Nucl. Phys. A **440**, 327 (1985).
[31] R. du Rietz, D. J. Hinde, M. Dasgupta, R. G. Thomas, L. R. Gasques, M. Evers, N. Lobanov, and A. Wakhle, Phys. Rev. Lett. **106**, 052701 (2011).
[32] R. du Rietz, E. Williams, D. J. Hinde, M. Dasgupta, M. Evers, C. J. Lin, D. H. Luong, C. Simenel, and A. Wakhle, Phys. Rev. C **88**, 054618 (2013).
[33] A. Wakhle, C. Simenel, D. J. Hinde, M. Dasgupta, M. Evers, D. H. Luong, R. du Rietz, and E. Williams, Phys. Rev. Lett. **113**, 182502 (2014).
[34] W. Loveland, arXiv:1411.4929v1 (2015).
[35] A. S. Umar and V. E. Oberacker, Phys. Rev. C **74**, 021601(R) (2006).
[36] K. Washiyama and D. Lacroix, Phys. Rev. C **78**, 024610 (2008).
[37] K. Wen, F. Sakata, Z.-X. Li, X.-Z. Wu, Y.-X. Zhang, and S.-G. Zhou, Phys. Rev. Lett. **111**, 012501 (2013).
[38] C. Simenel, R. Keser, A. S. Umar, and V. E. Oberacker, Phys. Rev. C **88**, 024617 (2013).
[39] C. Simenel, M. Dasgupta, D. J. Hinde, and E. Williams, Phys. Rev. C **88**, 064604 (2013).
[40] P. A. M. Dirac, Proc. Camb. Phil. Soc. **26**, 376 (1930).
[41] J. W. Negele, Rev. Mod. Phys. **54**, 913 (1982).
[42] Cédric Simenel, Eur. Phys. J. A **48**, 152 (2012).
[43] V. E. Oberacker, A. S. Umar, and C. Simenel, Phys. Rev. C **90**, 054605 (2014).

[44] A. S. Umar and V. E. Oberacker [Nucl. Phys. A (2015) (to be published)].
[45] C. Simenel and A. S. Umar, Phys. Rev. C **89**, 031601(R) (2014).
[46] G. Scamps, C. Simenel, and D. Lacroix, Phys. Rev. C **92**, 011602(R) (2015).
[47] P. M. Goddard, P. D. Stevenson, and A. Rios, arXiv:1504.00919 (2015).
[48] J. Blocki and H. Flocard, Phys. Lett. B **85**, 163 (1979).
[49] S. Stringari and D. Vautherin, Phys. Lett. B **88**, 1 (1979).
[50] A. S. Umar and V. E. Oberacker, Phys. Rev. C **71**, 034314 (2005).
[51] J. A. Maruhn, P. G. Reinhard, P. D. Stevenson, J. R. Stone, and M. R. Strayer, Phys. Rev. C **71**, 064328 (2005).
[52] T. Nakatsukasa and K. Yabana, Phys. Rev. C **71**, 024301 (2005).
[53] C. Simenel and P. Chomaz, Phys. Rev. C **68**, 024302 (2003).
[54] P.-G. Reinhard, P. D. Stevenson, D. Almehed, J. A. Maruhn, and M. R. Strayer, Phys. Rev. E **73**, 036709 (2006).
[55] P.-G. Reinhard, Lu Guo, and J. A. Maruhn, Eur. Phys. J. A **32**, 19 (2007).
[56] C. I. Pardi and P. D. Stevenson, Phys. Rev. C **87**, 014330 (2013).
[57] C. I. Pardi, P. D. Stevenson, and K. Xu, Phys. Rev. E **89**, 033312 (2014).
[58] E. B. Suckling and P. D. Stevenson, Europhys. Lett. **90**, 12001 (2010).
[59] I. Stetcu, A. Bulgac, P. Magierski, and K. J. Roche, Phys. Rev. C **84**, 051309(R) (2011).
[60] B. Avez and C. Simenel, Eur. Phys. J. A **49**, 76 (2013).
[61] G. Scamps and D. Lacroix, Phys. Rev. C **89**, 034314 (2014).
[62] P. Bonche, B. Grammaticos, and S. Koonin, Phys. Rev. C **17**, 1700 (1978).
[63] H. Flocard, S. E. Koonin, and M. S. Weiss, Phys. Rev. C **17**, 1682 (1978).
[64] C. Simenel, P. Chomaz, and G. de France, Phys. Rev. Lett. **86**, 2971 (2001).
[65] A. S. Umar, V. E. Oberacker, J. A. Maruhn, and P.-G. Reinhard, Phys. Rev. C **81**, 064607 (2010).
[66] L. Guo and T. Nakatsukasa, EPJ Web Conf. **38**, 09003 (2012).
[67] R. Keser, A. S. Umar, and V. E. Oberacker, Phys. Rev. C **85**, 044606 (2012).
[68] A. S. Umar, C. Simenel, and V. E. Oberacker, Phys. Rev. C **89**, 034611 (2014).
[69] X. Jiang, J. A. Maruhn, and S. Yan, Phys. Rev. C **90**, 064618 (2014).
[70] S. E. Koonin, K. T. R. Davies, V. Maruhn-Rezwani, H. Feldmeier, S. J. Krieger, and J. W. Negele, Phys. Rev. C **15**, 1359 (1977).
[71] C. Simenel, Phys. Rev. Lett. **105**, 192701 (2010).
[72] C. Simenel, Phys. Rev. Lett. **106**, 112502 (2011).
[73] A. S. Umar, V. E. Oberacker, and J. A. Maruhn, Eur. Phys. J. A **37**, 245 (2008).
[74] K. Sekizawa and K. Yabana, Phys. Rev. C **88**, 014614 (2013).
[75] G. Scamps and D. Lacroix, Phys. Rev. C **87**, 014605 (2013).
[76] K. Sekizawa and K. Yabana, Phys. Rev. C **90**, 064614 (2014).
[77] R. Balian and M. Véneroni, Phys. Lett. B **136**, 301 (1984).
[78] J. B. Marston and S. E. Koonin, Phys. Rev. Lett. **54**, 1139 (1985).
[79] P. Bonche and H. Flocard, Nucl. Phys. A **437**, 189 (1985).
[80] M. Tohyama and A. S. Umar, Phys. Lett. B **549**, 72 (2002).
[81] D. Lacroix and S. Ayik, Eur. Phys. J. A **50**, 95 (2014).
[82] C. Simenel, P. Chomaz, and G. de France, Phys. Rev. Lett. **93**, 102701 (2004).
[83] A. S. Umar and V. E. Oberacker, Phys. Rev. C **74**, 024606 (2006).
[84] D. J. Hinde, M. Dasgupta, J. R. Leigh, J. P. Lestone, J. C. Mein, C. R. Morton, J. O. Newton, and H. Timmers, Phys. Rev. Lett. **74**, 1295 (1995).
[85] Z. Liu, H. Zhang, J. Xu, Y. Qiao, X. Qian, and C. Lin, Phys. Lett. B **353**, 173 (1995).
[86] D. J. Hinde, M. Dasgupta, J. R. Leigh, J. C. Mein, C. R. Morton, J. O. Newton, and H. Timmers, Phys. Rev. C **53**, 1290 (1996).
[87] Y. T. Oganessian, V. K. Utyonkov, Y. V. Lobanov, F. S. Abdullin, A. N. Polyakov, I. V. Shirokovsky, Y. S. Tsyganov, G. G. Gulbekian, S. L. Bogomolov, B. N. Gikal, A. N. Mezentsev, S. Iliev, V. G. Subbotin, A. M. Sukhov, A. A. Voinov, G. V. Buklanov, K. Subotic, V. I. Zagrebaev, M. G. Itkis, J. B. Patin, K. J. Moody, J. F. Wild, M. A. Stoyer, N. J. Stoyer, D. A. Shaughnessy, J. M. Kenneally, P. A. Wilk, R. W. Lougheed, R. I. Il'kaev, and S. P. Vesnovskii, Phys. Rev. C **70**, 064609 (2004).
[88] G. N. Knyazheva, E. M. Kozulin, R. N. Sagaidak, A. Yu. Chizhov, M. G. Itkis, N. A. Kondratiev, V. M. Voskressensky, A. M. Stefanini, B. R. Behera, L. Corradi, E. Fioretto, A. Gadea, A. Latina, S. Szilner, M. Trotta, S. Beghini, G. Montagnoli, F. Scarlassara, F. Haas, N. Rowley, P. R. S. Gomes, and A. Szanto de Toledo, Phys. Rev. C **75**, 064602 (2007).
[89] D. J. Hinde, R. G. Thomas, R. du Rietz, A. Diaz-Torres, M. Dasgupta, M. L. Brown, M. Evers, L. R. Gasques, R. Rafiei, and M. D. Rodriguez, Phys. Rev. Lett. **100**, 202701 (2008).
[90] K. Nishio, H. Ikezoe, S. Mitsuoka, I. Nishinaka, Y. Nagame, Y. Watanabe, T. Ohtsuki, K. Hirose, and S. Hofmann, Phys. Rev. C **77**, 064607 (2008).
[91] A. S. Umar, M. R. Strayer, J. S. Wu, D. J. Dean, and M. C. Güçlü, Phys. Rev. C **44**, 2512 (1991).
[92] A. S. Umar and V. E. Oberacker, Phys. Rev. C **73**, 054607 (2006).
[93] J. A. Maruhn, P.-G. Reinhard, P. D. Stevenson, and A. S. Umar, Comp. Phys. Commun. **185**, 2195 (2014).
[94] E. Chabanat, P. Bonche, P. Haensel, J. Meyer, and R. Schaeffer, Nucl. Phys. A **635**, 231 (1998).
[95] P. A. M. Guichon, H. H. Matevosyan, N. Sandulescu, and A. W. Thomas, Nucl. Phys. A **772**, 1 (2006).
[96] P. Klüpfel, P.-G. Reinhard, T. J. Bürvenich, and J. A. Maruhn, Phys. Rev. C **79**, 034310 (2009).
[97] M. Kortelainen, T. Lesinski, J. More, W. Nazarewicz, J. Sarich, N. Schunck, M. V. Stoitsov, and S. Wild, Phys. Rev. C **82**, 024313 (2010).
[98] A. S. Umar, V. E. Oberacker, J. A. Maruhn, and P.-G. Reinhard, Phys. Rev. C **80**, 041601(R) (2009).
[99] J. R. Huizenga, A. N. Behkami, and L. G. Moretto, Phys. Rev. **177**, 1826 (1969).
[100] B. B. Back, R. R. Betts, J. E. Gindler, B. D. Wilkins, S. Saini, M. B. Tsang, C. K. Gelbke, W. G. Lynch, M. A. McMahan, and P. A. Baisden, Phys. Rev. C **32**, 195 (1985).

[101] J. G. Keller, B. B. Back, B. G. Glagola, D. Henderson, S. B. Kaufman, S. J. Sanders, R. H. Siemssen, F. Videbaek, B. D. Wilkins, and A. Worsham, Phys. Rev. C **36**, 1364 (1987).
[102] R. Vandenbosch and J. R. Huizenga, *Nuclear Fission* (Academic Press, New York, 1973).
[103] A. J. Sierk, Phys. Rev. C **33**, 2039 (1986).
[104] S. Cohen, F. Plasil, and W. J. Swiatecki, Ann. Phys. (NY) **82**, 557 (1974).
[105] C. Bottcher, M. R. Strayer, A. S. Umar, and P.-G. Reinhard, Phys. Rev. A **40**, 4182 (1989).
[106] A. Blazkiewicz, V. E. Oberacker, A. S. Umar, and M. Stoitsov, Phys. Rev. C **71**, 054321 (2005).